UCRL--93608

DE86 003471

COLLECTIVE VECTOR METHOD FOR CALCULATION OF E1 MOMENTS IN ATOMIC TRANSITION ARRAYS

S. D. Bloom
and
A. Goldberg

This paper was prepared for submittal to
Proceedings of the 3rd International Conference
on Radiative Properties of Hot Dense Matter
Williamsburg, VA
October 13-18, 1985

October 1985

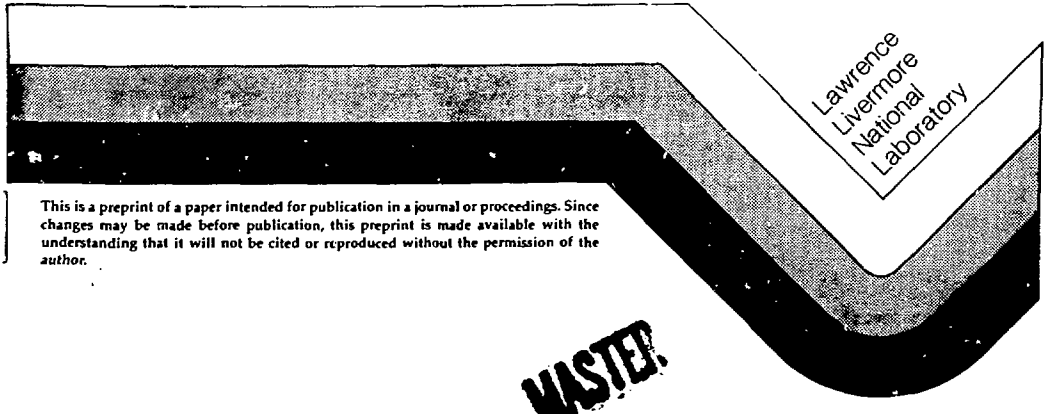

COLLECTIVE VECTOR METHOD FOR CALCULATION OF E1 MOMENTS IN ATOMIC TRANSITION ARRAYS

S. D. Bloom and A. Goldberg,

Lawrence Livermore National Laboratory
and
University of California-Davis, Department of Applied Science
Livermore, California 94550

ABSTRACT

The CV (collective vector) method for calculating E1 moments for a transition array is described and applied in two cases, herein denoted Z26A and Z26B, pertaining to two different configurations of iron VI. The basic idea of the method is to create a CV from each of the parent ("initial state") state-vectors of the transition array by application of the E1 operator. The moments of each of these CV's, referred to the parent energy, are then the rigorous moments for that parent, requiring no state decomposition of the manifold of daughter state-vectors. Since, in cases of practical interest, the daughter manifold can be orders of magnitude larger in size than the parent manifold, this makes possible the calculation of many moments higher than the second in situations hitherto unattainable via standard methods. The combination of the moments of all the parents, with proper statistical weighting, then yields the transition array moments from which the transition strength distribution can be derived by various procedures. We describe two of these procedures: (1) The well-known GC (Gram-Charlier) expansion in terms of Hermite polynomials, (2) The Lanczos algorithm or Stieltjes imaging method, also called herein the delta expansion. Application is made in the cases of Z26A (50 lines) and Z26B (5523 lines) and the relative merits and shortcomings of the two procedures are discussed.

I. Introduction

The use of collective state-vectors in getting transition strength distributions in many fermion systems is a standard technique in, for example, the RPA (random phase approximation) or the TDA (Tamm-Dancoff approximation). Here we describe a method where such state-vectors can, in principle, be used to obtain moments of arbitrary multipolarity to any order without making any approximations in the character of either the excitation or the correlations in the "ground" or parent state vector $|P\rangle$, as we shall term it here. As in any other method there are important limitations to this method. However our emphasis here is on the calculation of E1 (electric dipole) moments in atomic transition arrays where, as we shall show, these limitations are sufficiently loose so as to permit the study of complex atoms where ordinary diagonalization is impractical or other methods are limited to the evaluation of at most the second or, in some cases, the third moment.[1,2,3] For obvious reasons we call this the CV (collective vector) method. More general discussions of the method, in the context of nuclear applications, can be found in Refs. 4 and 5.

The definition of the CV is simple since, as usual, it requires only $|P\rangle$, the parent state vector and the E1 one-body operator, denoted by (E1). The action of (E1) on $|P\rangle$ produces $|CE1;P\rangle$, the collective E1 or daughter state vector,

$$|CE1;P\rangle \equiv (E1)|P\rangle \tag{1}$$

where it is to be noted that in general $|CE1;P\rangle$ is <u>not</u> an eigenvector of

the Hamiltonian, as $|P\rangle$ is. Note also that the model space for the daughter is much larger than for the parent by virtue of the extra particle/hole excitation produced by the E1 excitation (see below). The <u>total</u> strength for the transition, sometimes called the EUS, i.e. the energy unweighted sum, is given by,

$$(N_p)^2 = \langle CE1;P|CE1;P\rangle \qquad (2)$$

where the aptness of the symbol $(N_p)^2$ will become clear shortly. The centroidal moments $\mu_{Cn}(P)$ pertaining to each parent $|P\rangle$ are given by,

$$\mu_{Cn}(P) = \langle CE1;P|(H-\langle H\rangle)^n|CE1;P\rangle/(N_p)^2; \qquad n>1 \qquad (3)$$

where we now see that the total strength $(N_p)^2$ is the normalizing factor for the moments.

Besides the centroidal moments $\mu_{Cn}(P)$ we need the difference in energy between the parent state $|P\rangle$ and the centroid of $|CE1;P\rangle$ for which we use the symbol $\langle H1\rangle$,

$$\langle H1\rangle = [\langle CE1;P|H|CE1;P\rangle/(N_p)^2] - \langle P|H|P\rangle \qquad (4)$$

In principle we now have all that is needed to get the E1 strength distribution but we have not yet considered the spin projection dependence

explicitly. We will not give in all detail the equations with this feature included but give only the full expression for the E1 operator, which is very simple and will suffice to make the major arguments we need,

$$(E1) = \sum_{\mu} (E1)_{\mu} \tag{5}$$

where μ is the spin projection for the E1 operator. With Eq. (5) we can easily derive from Eq. (3) the familiar result for the n'th centroidal moment in factorized form,

$$\mu_n(P) = \sum_{J'M'} \langle J'M'|(E1)|JM\rangle^2 \langle J'|(H-\langle H\rangle)^n|J\rangle/(N_p)^2; \quad n>1 \tag{6}$$

where (JM, J'M') refer to (parent, daughter) spins and spin projections. Note that this result is independent of M due to Eq. (5) and the scalarity of H, which is to say μ_n is, as it must be, a scalar. Because of this a further simplification of Eq. (6) can be effected by the use of reduced matrix elements yielding,

$$\mu_n(P) = \sum \langle J'||E1||J\rangle^2 \langle J'|(H-\langle H\rangle^n)|J\rangle/(N_p)^2 \tag{7a}$$

$$(N_p)^2 = \sum \langle J'||E1||J\rangle^2 \tag{7b}$$

where all explicit spin-projection dependence has been eliminated. Note that there has been a slight change in the definition of the normalization $(N_p)^2$ (by a factor of (2J+1)) to conform to the use of reduced matrix elements.

It is Eqs. (7 a, b) and their practical evaluation via Eq. (3), which forms the basis for all the results to be described herein. The ingredients of the actual computation are the collective state vector $|CE1;P\rangle$, the parent state vector $|P\rangle$, and, of course, some means of calculating the various matrix elements required. In our case we have used the system of codes called VLADIMIR at LLNL to make all the required state-vectors as well as the Hamiltonian matrix elements. We will not discuss the VLADIMIR codes here except to note that they are couched entirely in terms of Fock space representation (2nd quantization) which, for the purposes involved here, is particularly useful since this makes it possible to deal with state-vectors and operators on a separate footing. [Two examples of the utility of this feature are in the implementation of Eqs. (1) and (5).] Further details may be found in Refs. 5 and 6.

II. Calculating the transition array

An atomic transition array generally has many parent states and we wish to utilize the set of moments $\mu_n(P)$ to describe the entire array. As we have seen only the state-vectors of the parent configuration are explicitly required, not those of the daughter. This makes for considerable computer economy, since, for example, in the two cases to be illustrated the parent configurations have 19 and 180 parent states, while the daughter configurations have respectively 128 and 3449 states.

The most common method for calculation of the transition array from the moments is the Gram-Charlier expansion.[7] This gives the strength function

$S_p(\omega)$ as a series in Hermite polynomials,

$$S_p(\omega) = (2/\pi)^{1/2} \sum_{n=0}^{\infty} c_n(P) \exp\left\{-(\omega-\langle H1\rangle)^2/2\mu_2(P)\right\} H_n\left(\frac{(\omega-\langle H1\rangle)}{[\mu_2(P)]^{1/2}}\right) \quad (8)$$

with $\langle H1\rangle$ given in Eq. (4) and $\mu_2(P)$ being the second centroidal moment of the array arising from $|P\rangle$. This expansion is exact if carried to infinite order, but as a practical matter is truncated at some value $n = N$, with the coefficients $c_0, c_1 \ldots c_N$ chosen so that the truncated expansion gives the first N+1 centroidal moments correctly ($\mu_0 = 1$, $\mu_1 = 0$).

This procedure will be illustrated in the next section, where a deficiency associated with the GC method will become apparent. It arises from the fact that the finite expansion allows negative values for $S_p(\omega)$. These negative excursions [$S_p(\omega)$ must of course be positive definite] can become quite significant, as will be seen.

A second procedure for synthesizing the transition strength distribution is the Stieltjes Imaging or delta expansion method. Here we use the Lanczos algorithm to implement the delta expansion. This has two main advantages: (1) it is more convenient computationally, about twice as fast as a straightforward evaluation of the moments, and (2) it yields a finite width to be associated with each line. The Lanczos procedure constructs a truncated set of basis vectors in the daughter model space, and, from these, generates a set of approximate eigenvectors $|e.v.\rangle$ of the daughter configuration. The energies of the approximate eigenvectors fix the delta expansion line energies, while the line intensities are the square of the projections of

$|CE1:P\rangle$ on these vectors. Finally, a computational width (as distinguished from a physical width) can be assigned to each line, to wit the energy fluctuation of that eigenvector, i.e.,

$$\Gamma^2 = \langle e.v.|H^2|e.v.\rangle - \langle e.v.|H|e.v.\rangle^2 \qquad (9)$$

Detailed discussions of the Lanczos method can be found in Refs. 6 and 10.

III. Results

In this section we give results for two calculations, labeled Z26A and Z26B, transition arrays for two parent configurations of Iron VI. The transition arrays correspond to

$$\text{Z26A:} \quad (3d)^3 \rightarrow (3d)^2(4p)$$
$$\text{Z26B:} \quad (3p)^5(3d)^4 \rightarrow (3p)^5(3d)^3(4f).$$

We discuss the Z26A case first. Here there are 4 parent energy levels and 19 distinct parent states in total J and energy. In both parent and daughter J takes on 6 distinct values, ranging from J = 1/2 to J = 11/2. This high degree of degeneracy results from the pure LS coupling used in both examples Z26A and Z26B. In this first example there are 50 transitions, distinct in energy, shown in Fig. 1a (with the exception of a few extremely weak lines).

This is an absorption spectrum save for a few lines at energies about -3eV. The arbitrary width of w = 0.06 eV was assigned to all lines for the sake of easier display, and also for consistency with the width used in the delta expansion (see below). Figure 1b exhibits the same spectrum, this time for positive transition energies only, with width w = 0.25 eV. This is a much smoother representation and, as will now be seen, is much more appropriate for comparison with the GC (Gram-Charlier) expansion results. In Fig. 2a we show the GC expansion results for 6 moments per parent, so that this represents a superposition of 19 GC expansions, each up to the 6th moment. We note the negative excursion at $\approx$ 12 eV, not too severe in this case. We have limited ourselves to the positive (absorption) spectrum only in this figure and also in Fig. 2b, which is an overlay of the GC result and the microscopic result with w = 0.25 eV (Fig. 1b). There is a fair correspondence between the broadened microscopic spectrum and the GC expansion except for such features as the peak at $\approx$ 8.5 eV. To obtain a better feeling as to how the GC method tries to fit simple spectra, we show in Fig. 3 the 6 moment result for one value of J, i.e., J = 11/2, which has only one parent and 3 lines (shown there with their proper strengths). For such spectra the GC method is completely inappropriate, but nonetheless this shows that the GC method would be equally inappropriate in cases where complex intermediate structure is of physical interest.

A more suitable method for studying structure in transition arrays is the delta expansion, the results for which are shown in Fig. 4. The delta expansion spectrum using 12 iterations per parent (corresponding to 23 moments per parent) is shown in Fig. 4a, while Fig. 4b shows that for 6 iterations per

parent (11 moments). In both each line was assigned a width either given by Eq. (8) or 0.06 eV, whichever was larger. The 12 iteration result is virtually indistinguishable from the microscopic result (Fig. 1a). All the weaker lines in the 6 iteration delta expansion spectrum have widths generated by the method itself, and comparison of this with the microscopic spectrum demonstrates nicely how the Lanczos method smoothes over the discrete structure when the algorithm has not reached complete convergence, as it had in the 12 iteration calculation.

Table 1 gives the overall moments for the entire Z26A array as calculated from the microscopic spectrum, the GC expansion, and the delta expansion. The GC moments depart substantially from the exact values by the 10th moment getting rapidly worse after this, despite the fact that the GC method generates 6 x 19 = 114 moments worth of information. (The slight deviations up to the 6th overall moment are due to neglect of the weak negative energy transitions.) The delta expansion moments agree within ≈25% with the microscopic values up to the 12th moment for the 6 iteration calculation with full widths for each line (see Sect. II). (For the 12 iteration result the agreement is marred only by the missing peaks in the microscopic spectrum.) In this case there are 19 x 11 = 209 moments worth of information, corresponding roughly to the 6 moment GC computation in that the computation times required are about the same, the delta expansion method being about a factor of 2 faster.

The delta expansion result at 6 iterations per parent with full widths for each line (see Sect. II) yields moments at significant variance with the microscopic values beyond the 12th moment (not shown in Table 1) due to the

distortion introduced by the intrinsic widths. However, Fig. 5 shows that the loss of some moment information is rather well compensated by the gain of the correct smoothed structural definition in both the weak and strong transition regions.

The Z26B case has 50 parent energy levels and 180 distinct parent states in both J and energy. J takes on 8 distinct values in the parent configuration (up to J = 15/2) and 9 for the daughter (up to J = 17/2). There are 5523 distinct transitions, shown in Fig. 5a with w = 0.10 eV and in Fig. 6b with w = 0.25 eV. As might be expected, no individual transitions are seen in Fig. 6b, but considerable "intermediate" structure remains. Figure 7 exhibits the overlay of Fig. 6b with the GC result using 6 moments per parent. The wings of the strength distribution are fitted quite well (except for the usual negative dips), but the center portion has a severe negative excursion, a result of the GC method trying to reproduce the double-humped structure of this particular spectrum. We show delta expansion results here only for the set of parent states with J = 15/2. There are 2 such, with about 150 daughters and about 100 lines. Figure 8a gives the Lanczos results with 12 iterations per parent, and with each line assigned a width of 0.2 eV. Assigning a small constant width ($\lesssim$ 0.2 eV) leaves the moments unaltered, and it is to be emphasized that the first 24 moments obtained this way are exact, i.e. as essentially as if calculated at zero width. Figure 8b exhibits the same delta expansion with the computational widths, Eq. (8), assigned to each line, and Fig. 8c overlays these two. In Fig. 8d, we show the overlay of Fig. 8a, and the 6 iteration delta expansion result with full width. As above the major effect of using the full widths is to smooth the resultant spectrum,

without greatly altering its general shape. One does not really need the full 12 iterations to obtain a substantially correct strength distribution. Table II gives the values for the moments for the J = 15/2 parent manifold, for these various computations. Beyond the 6th moment, those obtained from the full width spectra for both 6 and 12 iterations diverge from the correct moments. This, as before, is a distortion due to the broadening procedure. Nonetheless, as before, the shape of the spectrum is much better retained by the delta expansion method than by the GC method.

IV. Conclusion

Although the second test case (Z26B) is not complete, a number of firm conclusions may be drawn. First the general procedure described here forms a practical method for characterizing atomic transition arrays, and is especially applicable when the array contains more than 5000 lines (essentially the limiting number for use of purely microscopic methods). It is to be emphasized that although intermediate coupling and/or configuration interaction effects have not been considered in these test cases, such effects can be included with no additional work and with no increase in computer time.

Secondly, the use of a Gram-Charlier type of description of the array seems to be useful only for the gross overall features determined from the first few moments. Sixth (or higher) order Gram-Charlier expansions result in unphysical negative strength distributions. In any case, the GC expansion as a practical matter appears incapable of giving any structure in the transition array. The Lanczos delta-expansion on the other hand is positive definite everywhere and can be used to give detailed structure in the array,

unambiguously giving strength distributions quite similar to the microscopically computed array. This clearly seems the preferred method when 4 or more moments are known.

One difficulty of our method is the fact that as of now it is executed for each of the parent states. Test case Z26B has 180 such parent states, and interesting arrays could have many more. We intend then to develop a Monte Carlo-Lanczos procedure to simulate the states of the parent configuration. That is, we choose a random starting vector and then use the Lanczos method to construct approximate eigenstates within the parent manifold. This procedure will considerably shorten the computation and allow application to much larger parent manifolds, for example configurations in the N-shell.

ACKOWLEDGEMENTS

The authors are grateful to K. Reed for providing the microscopic strength distribution for test case Z26A. We also must thank S. M. Grimes, J. D. Anderson, and B. Rozsnyai for a number of enlightening conversations. Work performed under the auspices of the U.S. Department of Energy by Lawrence Livermore National Laboratory under contract #W-7405-Eng-48.

Table I Overall moments up to the 12th moment, for case Z26A, as computed from microscopic spectrum, etc. The overall moments are the weighed sums of the moments of each parent (see Sect. I). The units are arbitrary. The exponents are given in parentheses. See Sect. III.

$$\mu_n = \sum_P (2J_P+1)\ \mu_n(P)$$

		GC	Lanczos (full widths)	
n	Microscopic	$N_{mom} = 6$	$N_{it} = 6$	$N_{it} = 12$
2	7.65	7.73	7.77	7.74
3	-1.55 (1)	-1.59 (1)	-1.64 (1)	-1.62 (1)
4	2.59 (2)	2.62 (2)	2.70 (2)	2.66 (2)
5	-1.29 (3)	-1.26 (3)	-1.38 (3)	1.34 (3)
6	1.80 (4)	1.68 (4)	1.90 (4)	1.85 (4)
7	-1.34 (5)	-1.16 (5)	-1.44 (5)	-1.36 (5)
8	1.76 (6)	1.61 (6)	1.89 (6)	1.78 (6)
9	-1.62 (7)	-1.61 (7)	1.76 (7)	-1.61 (7)
10	2.04 (8)	2.57 (8)	2.23 (8)	2.03 (8)
11	-2.08 (9)	-3.63 (9)	-2.32 (9)	-2.05 (9)
12	2.55 (10)	6.34 (10)	2.86 (10)	2.50 (10)

Table II Moments for case Z26B for the parent state manifold with J = 15/2. There are 2 parent states and approximately 150 daughter states that are connected to these parents by E1 transitions. See Sect. III.

	Lanczos			GC
n	N_{it} = 12	N_{it} = 12	N_{it} = 6	N_{mom} = 6
	ω=0.2 ev (correct)	full width	full width	
2	7.46	8.25	8.57	7.44
3	-2.38 (1)	-2.42 (1)	-1.75 (1)	-2.34 (1)
4	4.06 (2)	4.55 (2)	5.00 (2)	4.04 (2)
5	-3.85 (3)	-4.05 (3)	-3.62 (3)	-3.81 (3)
6	4.78 (4)	5.52 (4)	5.71 (4)	4.73 (4)
7	-5.60 (5)	-6.58 (5)	-5.93 (5)	-4.21 (5)
8	6.91 (6)	9.02 (6)	8.41 (6)	5.76 (6)
9	-8.65 (7)	-1.26 (8)	-1.04 (8)	-6.04 (7)
10	1.13 (9)	1.94 (9)	1.54 (9)	7.97 (8)
11	-1.54 (10)	-3.28 (10)	-2.31 (10)	-1.06 (10)
12	2.28 (11)	6.19 (11)	4.11 (11)	1.29 (11)

References

1. A. L. Merts, "Moment Methods in Many-Fermion Systems", edited by B. J. Dalton, S. M. Grimes, J. P. Vary, and S. A. Williams, p. 81, 1979.

2. C. Bauche-Arnoult, J. Bauche, and M. Klapisch, Phys. Rev. A 20, 2424 (1979).

3. J. Bauche, et al, Phys. Rev. A, 28, 829 (1983).

4. S. D. Bloom and R. F. Hausman, Jr., see Ref. 1, p. 151, 1979.

5. S. D. Bloom, Progress in Particle and Nuclear Physics, 11, 505 (1983).

6. R. F. Hausman, Jr., "A Vector Method for Large-Scale Configuration Interaction Problems", UCRL-52178, 1976; unpublished.

7. M. Kendall and A. Stuart, The Advanced Theory of Statistics, MacMillen (New York) 1977, pp 168-175.

8. P. W. Langhoff, see Ref. 1, p. 191, 1979.

9. R. R. Whitehead, see Ref. 1, p. 235, 1979.

10. R. R. Whitehead et al, Advances in Nuclear Physics; Editors, M. Baranger and E. Vogt, Plenum, N.Y., 1977, p. 123.

FIGURE CAPTIONS

Fig. 1-a: *Microscopic spectrum for Z26A with a width w = 0.06 eV, for 48* lines (unnormalized). This is an absorption spectrum except for the two negative energy lines at ~ -3eV. See Sect. III.

Fig. 1-b: Same as Fig. 1-a except that w = 0.25 eV. and the negative energy part of the spectrum is not displayed. Also this distribution is normalized to unity. See Sect. III.

Fig. 2-a: The Gram-Charlier (GC) expansion for Z26A with 6 moments per parent (19 parents). See Sect. III for a fuller discussion.

Fig. 2-b: Overlay of Figs. 2-a and 1-b. Note that the GC representation has significant contributions from the off-scale (unphysical) energy region.

Fig. 3: Case Z26A. Overlay of the 6 moment GC expansion and the 3 microscopic strengths originating from the single parent with J = 11/2. See Sect. III for a fuller discussion.

Fig. 4-a: Delta expansion result for Z26A with 12 iterations per parent, with minimum width w = 0.06 eV. See Sect. III.

Fig. 4-b: Same as Fig. 4-a, but with 6 iterations per parent.

Fig. 5: Overlay of case Z26A microscopic spectrum, Fig. 1-a, and delta expansion, Fig. 4-b. See Sect. III.

Fig. 6-a: Microscopic spectrum for test case Z26B, with each line given a width w = 0.1 eV. This emission spectrum contains 5523 lines, mainly unresolved, even at 0.1 eV width.

Fig. 6-b: Same as Fig. 6-a, but with width w = 0.25 eV. There are no unresolved lines using this width.

Fig. 7: Overlay of GC results for Z26B with 6 moments per parent (180 parents) with the microscopic spectrum of Fig. 6-b. The extreme negative excursion at the center of the spectrum arises from the attempt of the GC method to reproduce the double peaked structure of the true spectrum. See Sect. III.

Fig. 8-a: Delta expansion result (for Z26B) for the two parent states with J = 15/2. The computation used 12 iterations per parent, and each line was given a width w = 0.2 eV. See Sect. III.

Fig. 8-b: Same as Fig. 8-a, except each line was given its full intrinsic width as discussed in Sect. III.

Fig. 8-c: Overlay of Figs. 8-a and 8-b.

Fig. 8-d: Overlay of Fig. 8-a and the delta expansion with full width but with 6 (rather than 12) iterations per parent.

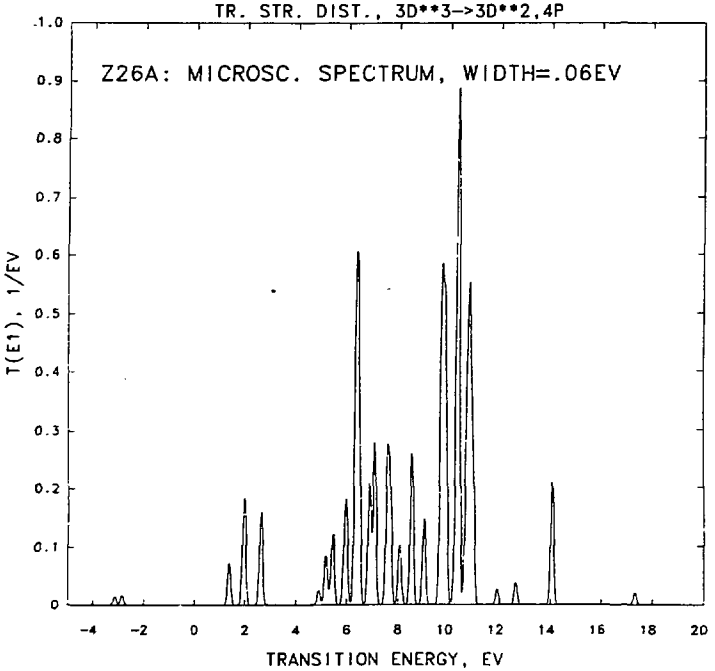
TR. STR. DIST., 3D**3->3D**2,4P
Z26A: MICROSC. SPECTRUM, WIDTH=.06EV
T(E1), 1/EV
1.0
0.9
0.8
0.7
0.6
0.5
0.4
0.3
0.2
0.1
0
-4
-2
0
2
4
6
8
10
12
14
16
18
20
TRANSITION ENERGY, EV

Figure 1a

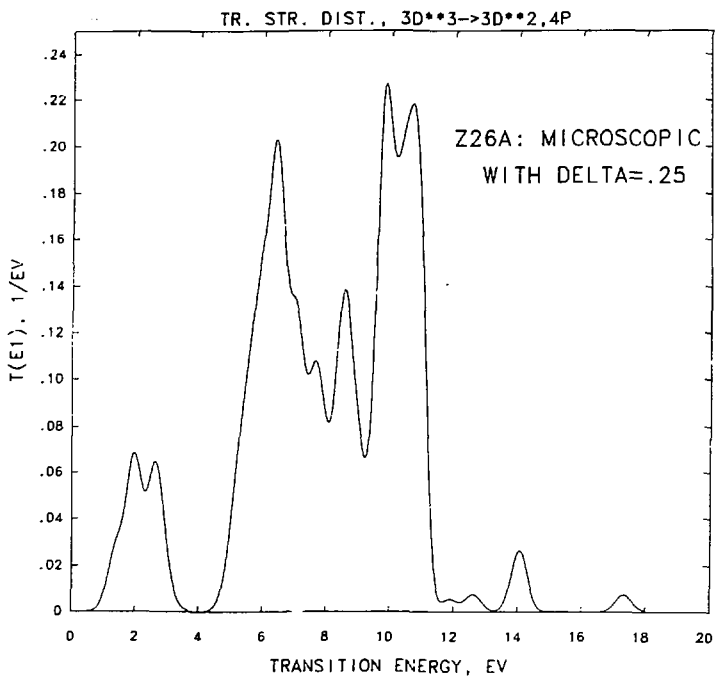
TR. STR. DIST., 3D**3->3D**2,4P
Z26A: MICROSCOPIC
WITH DELTA=.25
T(E1), 1/EV
.24
.22
.20
.18
.16
.14
.12
.10
.08
.06
.04
.02
0
0
2
4
6
8
10
12
14
16
18
20
TRANSITION ENERGY, EV

Figure 1b

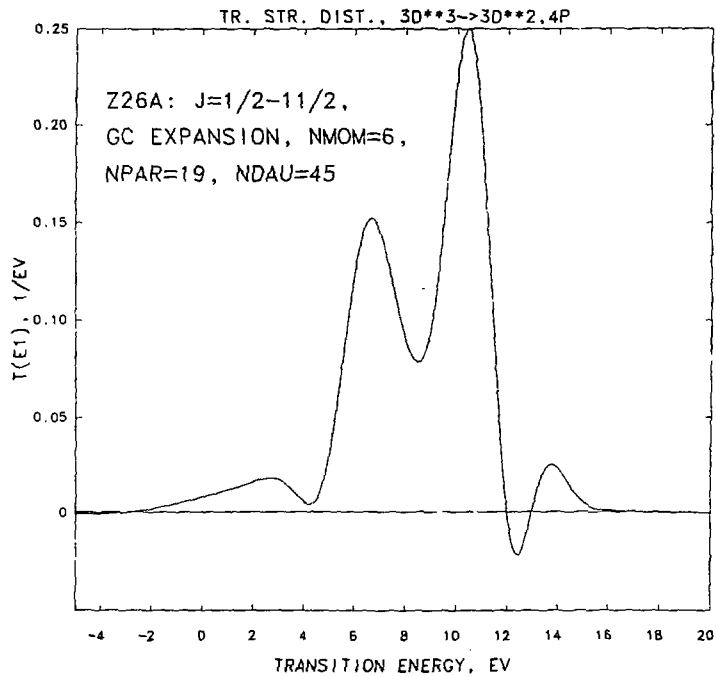
TR. STR. DIST., 3D**3->3D**2.4P
Z26A: J=1/2-11/2,
GC EXPANSION, NMOM=6,
NPAR=19, NDAU=45
T(E1), 1/EV
0.25
0.20
0.15
0.10
0.05
0
-4
-2
0
2
4
6
8
10
12
14
16
18
20
TRANSITION ENERGY, EV

Figure 2a

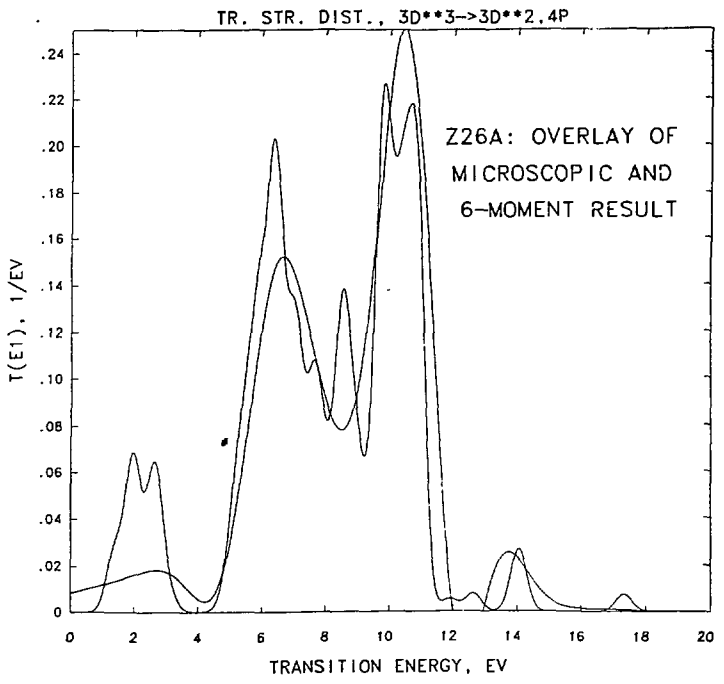
TR. STR. DIST., 3D**3->3D**2,4P
Z26A: OVERLAY OF
MICROSCOPIC AND
6-MOMENT RESULT
T(E1), 1/EV
.24
.22
.20
.18
.16
.14
.12
.10
.08
.06
.04
.02
0
0
2
4
6
8
10
12
14
16
18
20
TRANSITION ENERGY, EV

Figure 2b

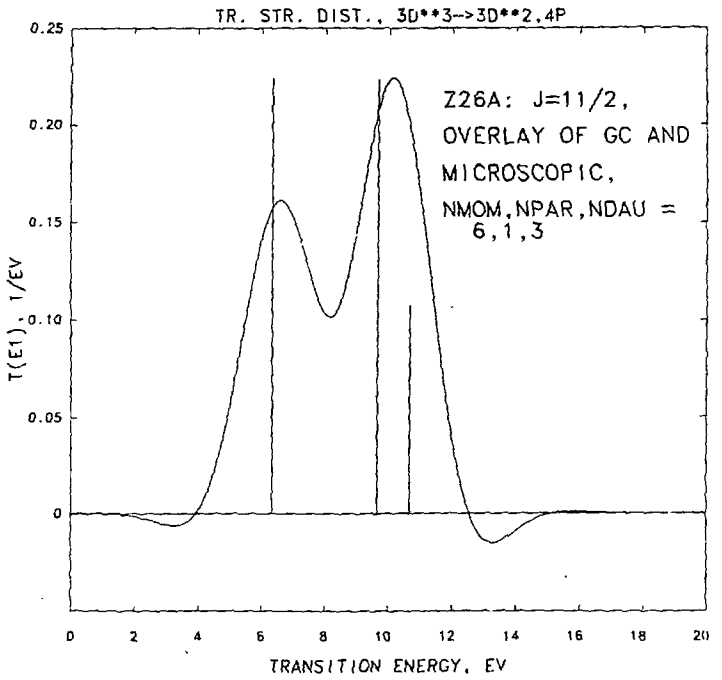
TR. STR. DIST., 3D**3-->3D**2.4P
Z26A: J=11/2,
OVERLAY OF GC AND
MICROSCOPIC,
NMOM,NPAR,NDAU =
6,1,3
T(E1), 1/EV
0.25
0.20
0.15
0.10
0.05
0
0
2
4
6
8
10
12
14
16
18
20
TRANSITION ENERGY, EV

Figure 3

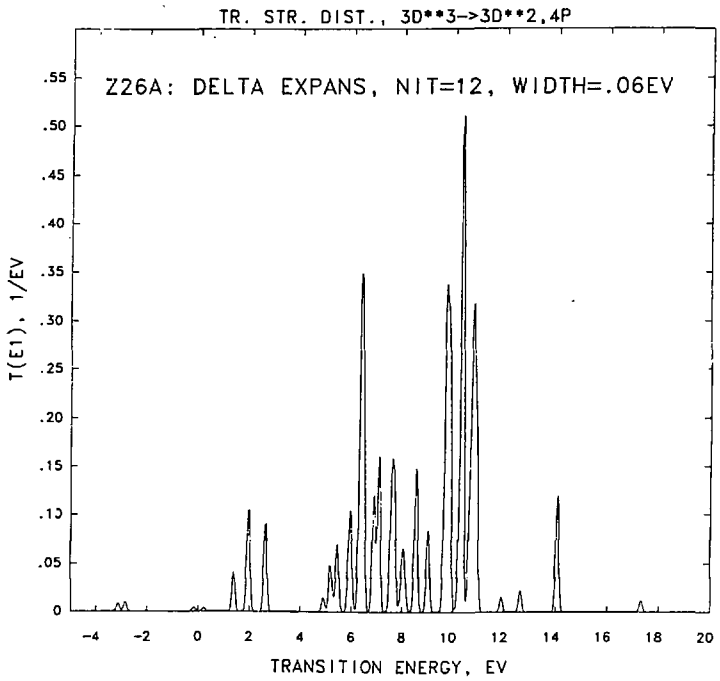
TR. STR. DIST., 3D**3->3D**2,4P
Z26A: DELTA EXPANS, NIT=12, WIDTH=.06EV
T(E1), 1/EV
.55
.50
.45
.40
.35
.30
.25
.20
.15
.10
.05
0
-4
-2
0
2
4
6
8
10
12
14
16
18
20
TRANSITION ENERGY, EV

Figure 4a

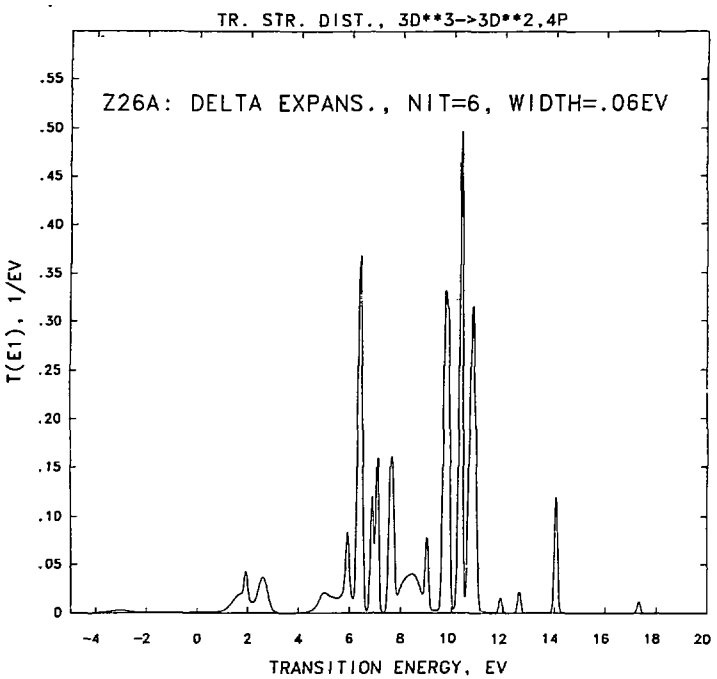
TR. STR. DIST., 3D**3->3D**2,4P
Z26A: DELTA EXPANS., NIT=6, WIDTH=.06EV
T(E1), 1/EV
.55
.50
.45
.40
.35
.30
.25
.20
.15
.10
.05
0
-4
-2
0
2
4
6
8
10
12
14
16
18
20
TRANSITION ENERGY, EV

Figure 4b

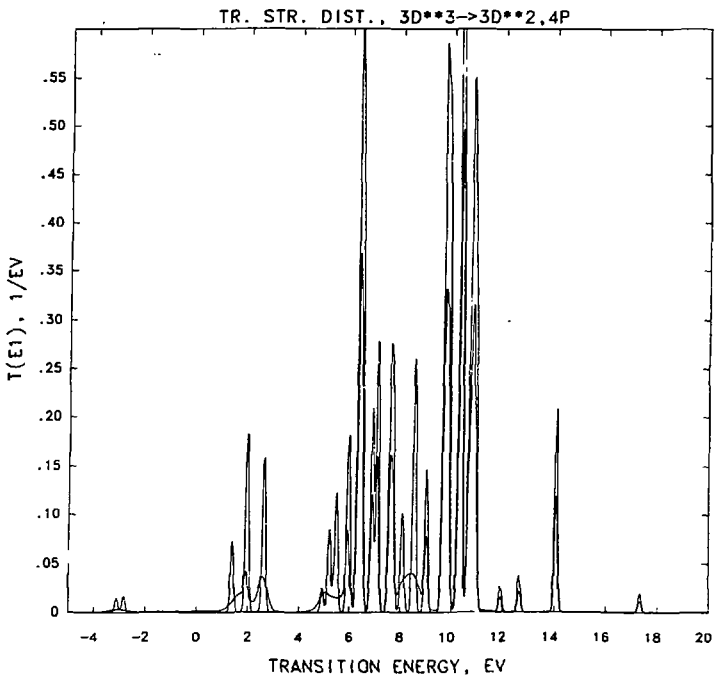
TR. STR. DIST., 3D**3->3D**2,4P
T(E1), 1/EV
.55
.50
.45
.40
.35
.30
.25
.20
.15
.10
.05
0
-4
-2
0
2
4
6
8
10
12
14
16
18
20
TRANSITION ENERGY, EV

Figure 5

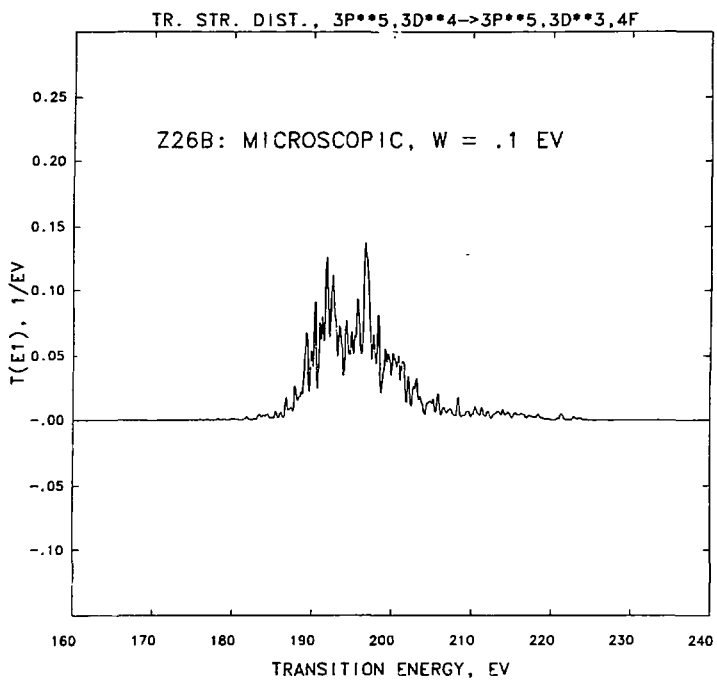
TR. STR. DIST., 3P**5,3D**4->3P**5,3D**3,4F
Z26B: MICROSCOPIC, W = .1 EV
T(E1), 1/EV
0.25
0.20
0.15
0.10
0.05
-.00
-.05
-.10
160
170
180
190
200
210
220
230
240
TRANSITION ENERGY, EV

Figure 6a

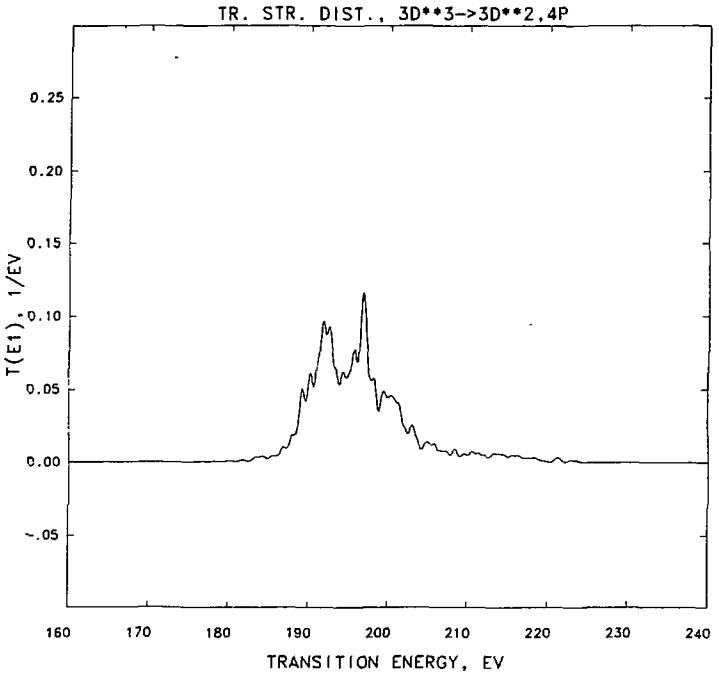
TR. STR. DIST., 3D**3->3D**2,4P
T(E1), 1/EV
0.25
0.20
0.15
0.10
0.05
0.00
-.05
160
170
180
190
200
210
220
230
240
TRANSITION ENERGY, EV

Figure 6b

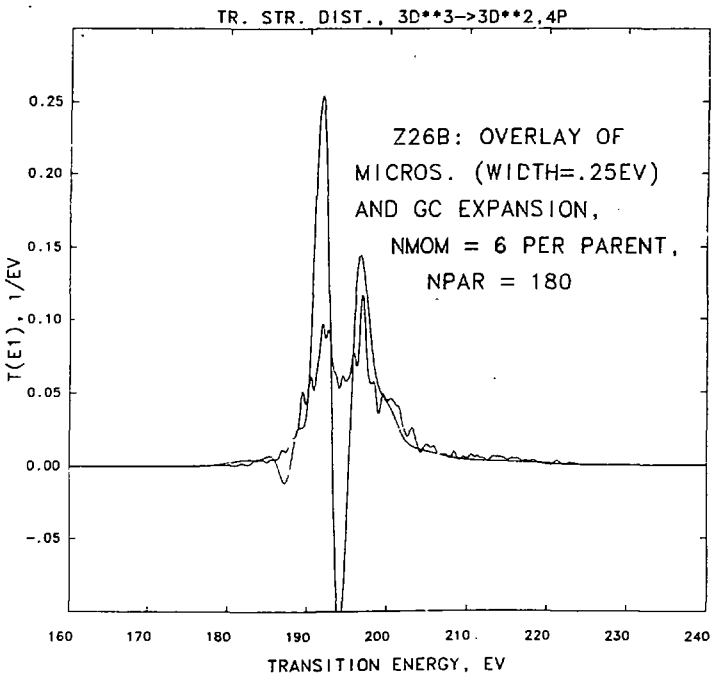
TR. STR. DIST., 3D**3->3D**2,4P
Z26B: OVERLAY OF
MICROS. (WIDTH=.25EV)
AND GC EXPANSION,
NMOM = 6 PER PARENT,
NPAR = 180
T(E1), 1/EV
0.25
0.20
0.15
0.10
0.05
0.00
-.05
160
170
180
190
200
210
220
230
240
TRANSITION ENERGY, EV

Figure 7

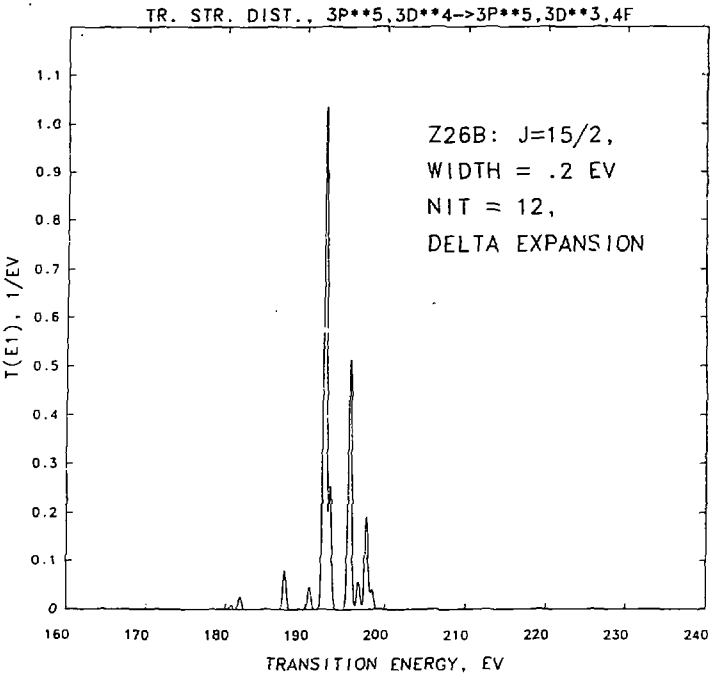
TR. STR. DIST., 3P**5,3D**4->3P**5,3D**3,4F
Z26B: J=15/2,
WIDTH = .2 EV
NIT = 12,
DELTA EXPANSION
T(E1), 1/EV
1.1
1.0
0.9
0.8
0.7
0.6
0.5
0.4
0.3
0.2
0.1
0
160
170
180
190
200
210
220
230
240
TRANSITION ENERGY, EV

Figure 8a

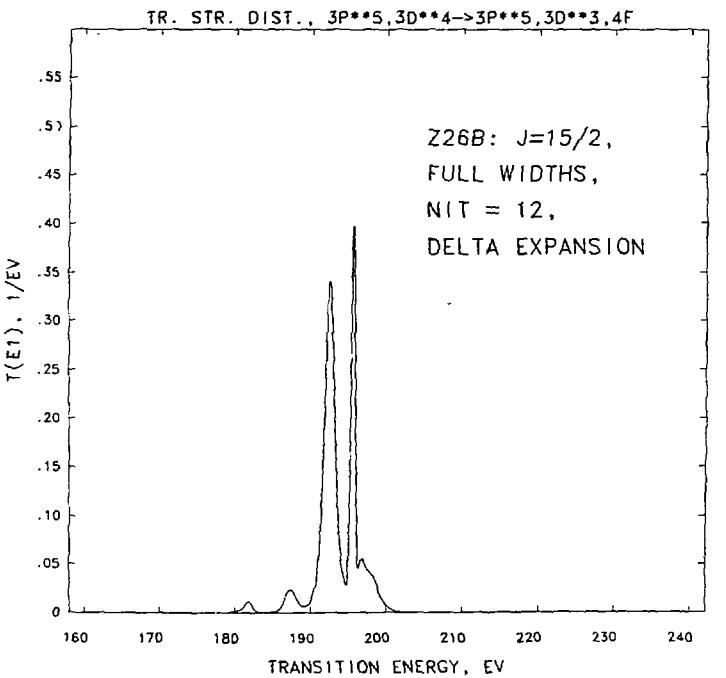
TR. STR. DIST., 3P**5,3D**4->3P**5,3D**3,4F
Z26B: J=15/2,
FULL WIDTHS,
NIT = 12,
DELTA EXPANSION
T(E1), 1/EV
.55
.50
.45
.40
.35
.30
.25
.20
.15
.10
.05
0
160
170
180
190
200
210
220
230
240
TRANSITION ENERGY, EV

Figure 8b

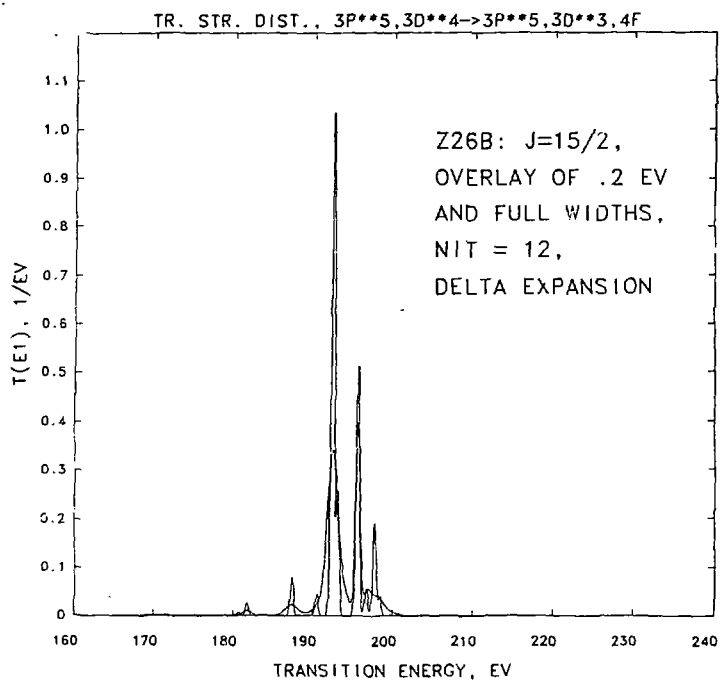
TR. STR. DIST., 3P**5,3D**4->3P**5,3D**3,4F
Z26B: J=15/2,
OVERLAY OF .2 EV
AND FULL WIDTHS,
NIT = 12,
DELTA EXPANSION
T(E1), 1/EV
0
0.1
0.2
0.3
0.4
0.5
0.6
0.7
0.8
0.9
1.0
1.1
160
170
180
190
200
210
220
230
240
TRANSITION ENERGY, EV

Figure 8c

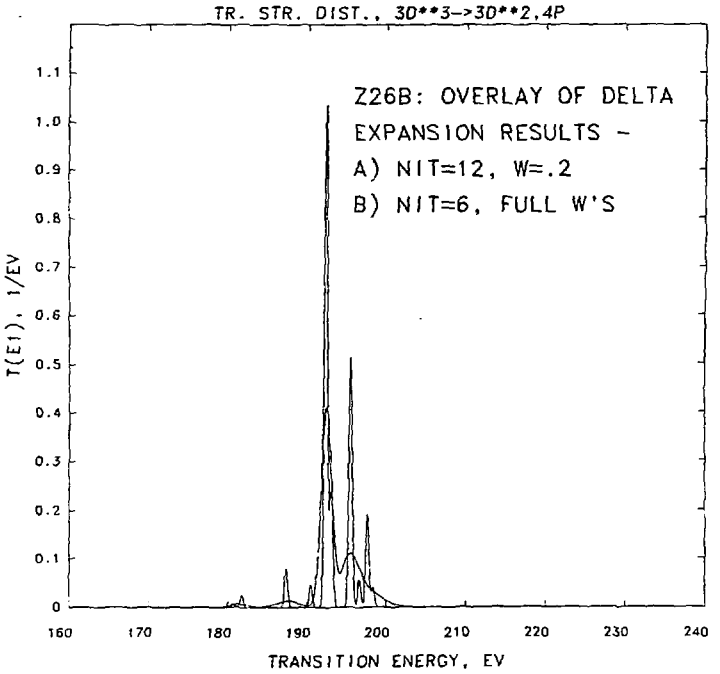

Figure 8d

DISCLAIMER